Origin of giant anisotropy in synthesized Ba pentaborates

P. Smok,[1] I. V. Kityk,[1] K. J. Plucinski,[2] and J. Berdowski[1]
[1]*Institute of Physics WSP, Al.Armii Krajowej 13/15, Częstochowa, Poland*
[2]*Military University of Technology, 00-908, ul. Kaliskiego 2, Warsaw, Poland*
(Received 30 July 2001; revised manuscript received 4 January 2002; published 22 April 2002)

The electronic structure, charge density distribution, and linear-optical properties of the highly anisotropic crystal $Ba[B_5O_8(OH)_3]$ (BaBOH) are calculated using a self-consistent norm-conserving pseudopotential method within a framework of local-density approximation theory. Large anisotropies of the band energy gap (5.22 eV for the **E**||**b**, 5.67 eV for the **E**||**c**) and giant birefringence (up to 0.17) are obtained. Comparison of the theoretically calculated and experimentally measured polarized spectra of the imaginary part of dielectric susceptibility ε_2 shows good agreement. It is shown that the anisotropy of the charge density distribution and the optical spectra is caused prevailingly by the huge anisotropy between $2p_z$ B$-2p_z$ O and $2p_{y,x}$ B$-2p_{y,x}$ O bonding orbitals. The observed anisotropy in BaBOH is principally different from the β-BaB_2O_4 (BBO) single crystals. In the BaBOH single crystals the anisotropic optical and charge density distribution is caused by a different projection of the orbitals originating from particular borate clusters on the particular crystallographic axes, contrary to the BBO, where the anisotropy is originated mainly due to different local site symmetry of the oxygen within the borate planes. The observed anisotropy is analyzed within the band energy approach and space charge density distribution.

DOI: 10.1103/PhysRevB.65.205103 PACS number(s): 71.15.Dx, 71.20.Ps

I. INTRODUCTION

Recently one can observe an increasing interest in borate crystals.[1–7] They are used in various quantum electronic and nonlinear optical devices. Particularly they are widely applied as materials for laser modulators, deflectors, frequency generators, and optical parametric oscillators. They possess excellent second-order nonlinear optical susceptibilities, a wide window of transparency (up to the VUV spectral range), and a high laser power damage threshold.

Another interesting application of the mentioned crystals is connected with the search for dielectrics possessing large anisotropy of the optical properties. The latter is particularly important for the creation of polarized optical filters and passive laser *Q* switchers. In order to produce materials possessing simultaneously good nonlinear optical properties and large anisotropy, it is necessary to understand the relationship between the electronic structure, spectroscopic properties, charge density distribution, and principal chemical bonds. Among the borates possessing anisotropy studied are β-BaB_2O_4 (BBO) and LiB_3O_5 (LBO) single crystals. Analyzing the previous works devoted to their band structures[8,9] one can see that the variation by the cationic subsystem as well as by the coordination positions of oxygen within borate rings allow one to operate by the degree of anisotropy in the charge density distribution and the corresponding optical and dielectric constants.

During the search for highly anisotropic borates and analyzing the crystallochemistry of different borates we have focused on pentaborates[10] possessing large structural anisotropy in different crystallographic directions. Of particular interest are $Ba[B_5O_8(OH)_3]$ (BABOH) single crystals (space group *P-I*). These crystals possess discrete tetrahedral $B(OH)_4$ groups and subsequent refinement of these structures has localized positions of the H atoms.[10,11] The BABOH single crystals have a relatively complicated crystallographic structure, with different configurations of anionic borate complexes and Ba polyhedra, different forms of Ba coordination and distortions of *B* tetrahedra, triangles, etc. Typical crystalline units of the BABOH crystal are presented in Fig. 1. Comparing with other anisotropic borates (such as BBO, LBO, GdCOB, CLBO)[3,8,9] (where anisotropy is originated from the different oxygen localization within the borate ring and different interlayer stacking) in the case of the BaBOH the anisotropy is caused by the above mentioned complicated structural configuration of particular

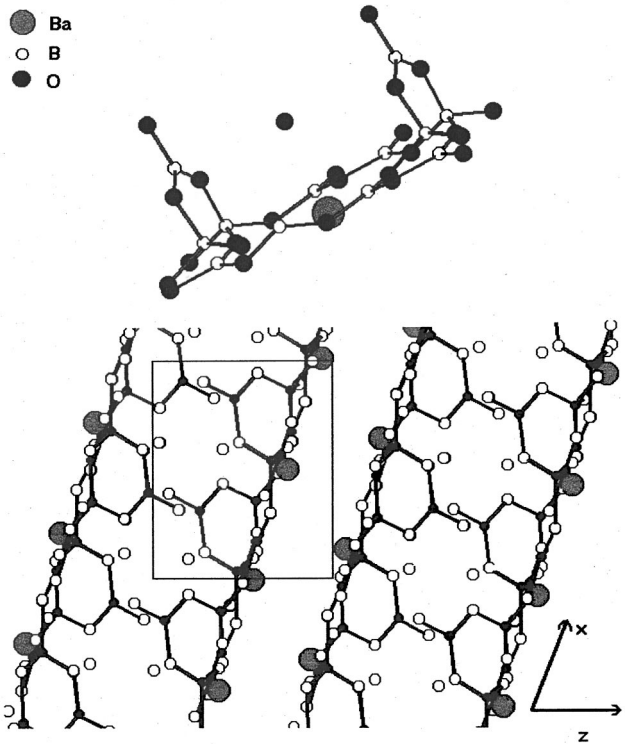

FIG. 1. General crystallochemistry of the BABOH crystalline unit.

clusters with respect to the crystallographic axes.

Thus the charge density anisotropy of the BABOH is expected to be substantially higher than in the case of the BBO or LBO and it would be interesting to consider the influence of this extremely anisotropic crystallochemistry structure on the band structure (BS), charge density distribution, and corresponding optical properties. In addition, the BaBOH's have only two molecules in crystal units that allows one to avoid many overlapping bands.

For the reasons presented above we have chosen the BaBOH single crystals as a model of highly anisotropic crystals for the investigation of the influence of the mentioned crystallographic anisotropy on the BS, charge density distribution, and polarized optical spectra. The optical spectra and charge density distribution of the BBO and LBO crystals have been well studied[8,9] and we will compare their band structure features with the ones for the BABOH.

Further investigations, materials engineering modifications, and applications of these materials are, however, strongly hampered by the lack of systematic studies of their BS and, particularly, the density of electronic band states directly connected with the chemical bonds. The latter parameters are necessary for the evaluation of microscopic features such as dipole moments, effective carrier masses, and optical dispersion determining nonlinear optical parameters. Among the different calculation techniques, the norm-conserving pseudopotential[12] scheme seems to be more useful for describing optical properties of borates.[3]

The observed anisotropy is discussed both within the band structure approach, as well as within the particular bonding-antibonding orbitals. To verify the calculated BS, we compared the spectral dispersion of the imaginary part of dielectric susceptibility $\varepsilon_2(E)$ calculated on the basis of the BS calculations and the one measured by ellipsometric measurements for different light polarizations.

In Sec. II, parameters of BaBOH crystal's and their preparation for ellipsometric measurements are presented. The BS calculation is given in Sec. III. Results of the charge density distribution, together with the BS diagrams and optical spectra are presented in Sec. IV. The origin of the anisotropy in the $\varepsilon_2(E)$ spectra within a framework of BS is discussed in Sec. V.

II. EXPERIMENTAL METHODS

A. Specimen's preparation

The investigated BaBOH crystals were grown by a method described in Refs. 10, 11. They had sizes of $3\times3\times5$ mm^3. Monitoring of the BaBOH single crystal structure was done using a DRON 5.0 x-ray diffractometer. The powder diffractometry showed that the space group of the BABOH crystals is triclinic $P-1$ with lattice parameters $a=6.785$ A, $b=6.831$ A, $c=10.6296$ A ($Z=2$). Specimen's homogeneity was monitored using an optical polarization method. We found that deviation from homogeneity is less than 3.6% throughout the specimen's surface. Due to the layered structure, the preparation of mirrorlike specimens in the $\langle 011\rangle$ crystallographic plane presents no difficulties.

B. Measurement technique

Ellipsometric measurements were made using a Seya-Numioka monochromator within the 3–25 eV spectral range. The specimen surfaces (3×3 mm) were cleaved along the mirrorlike (**bc**) planes and did not require an additional treatment.

The precision of the $\varepsilon_2(E)$ evaluation was equal to about 3.6%. The specimens were cleaved in a vacuum of about 10^{-4} Torr. The grating monochromator enabled us to make measurements of $\varepsilon_2(E)$ with a spectral resolution up to 2 nm/mm. MgF_2 polarizers were used for as VUV-light polarizers. The incident UV beam angle was changed within the range 2°–47° with respect to the normal of the cleaved plane. The computing program XC-130P was used for evaluations of $\varepsilon_2(E)$ tensor components at different incident angles. A photomultiplier operating in the single quantum calculation regime was used for detection of reflection light signal.

The fundamental absorption measurements were done using a polarized spectrophtometer within the 200–350 nm (spectral resolution about 4 A/mm). The refractive indices were measured using the spectroscopic method of Obreimow with a precision better than 10^{-3} for two wavelengths $\lambda=337$ nm and $\lambda=633$ nm.

III. CALCULATION PROCEDURE

The norm-conserving pseudopotential calculations were done using the plane wave (PW) basis set. Initial structural parameters were taken from Refs. 10, 11.

During the pseudopotential calculation the following atomic wave functions were included: the occupied $2s^2$, $2p^1$B, $2s^2 2p^4$O, $1s^1$H, $5p^6$Ba, $4d^{10}$Ba, $6s^2$Ba valence orbitals and excited unoccupied $3s$, $3p$B, $3s$, $3p$O, $2s$H, $6p$Ba orbitals.

The basic matrix elements of the secular equation were calculated analytically similarly to those described in Refs. 13, 14. Calculations were done for 78 **k** points of the Brillouin zone (BZ). Electron screening effects were taken into account using parametrized Perdew-Zunger[15] and Ceperley-Alder expressions.[16] The Chadi-Cohen method[17] was used for calculations of the pseudoelectron charge density distribution of valence electrons. This method was used to construct the pseudowave charge density function of electrons that is necessary for numerical evaluations of electron-electron and electron-exchange interactions.

Acceleration of the iteration convergence was achieved by transferring 70% of the $(m-1)$-th iteration result to the mth iteration. The following condition was taken as a criterion of self-consistency

$$|\rho_{\mathrm{out},m}-\rho_{\mathrm{inp},m}|<\varepsilon \tag{1}$$

after the mth iteration step. We have assumed that $\varepsilon=1\%$. The energy eigenvalues were stable up to 0.0012 eV and the total energy up to 0.0010 eV. This one corresponded to the number of plane waves varying within 400–568 depending on the BZ points. The numerical evaluations of the charge

density function terms were carried out using a numerical tetrahedral method with an increment equal to about 0.0008 eV.

The calculation of the imaginary part of dielectric susceptibility $\varepsilon_2(E)$ was done using the expression

$$\varepsilon_{2z,y}(E)=\frac{2\pi e^2}{mE}\int d^3\mathbf{k}\sum_{nl}\langle\psi_n(\mathbf{k},\mathbf{r})|\nabla_{z,y}|\psi_l(\mathbf{k},\mathbf{r})\rangle^2 n_l(\mathbf{k})$$
$$\times[1-n_n(\mathbf{k})]\delta[E_n(\mathbf{k})-E_l(\mathbf{k})-E],$$

where $\psi_n(k,r)$, $\psi_l(k,r)$ are basic plane-wave wave functions for the valence band and conduction bands, respectively. $n_l(k)$ and $n_n(k)$ are the occupations of the *l,n* band states, respectively. *z,y* are the chosen light polarizations with respect to the **c,b**-crystallographic direction.

The dipole optical transition momenta were calculated within 60 **k** points in part of the $\frac{1}{2}$th Brillouin zone. All the summations were performed using tetrahedral methods.

IV. RESULTS

Our calculations showed that for achievement of sufficient total energy and eigenstate convergence, it is necessary to have a cutoff energy level equal to about 46 Ry. During the calculations we also varied the starting structural parameters **a**, **b**, and **c** (up to $\pm 5\%$) comparing with the initial experimentally measured structure[10,11] in order to find the total energy minimum. Our calculations showed that the optimized crystalline structure corresponds to the lattice parameters **a**=6.7337 A, **b**=6.7769 A, and **c**=10.5779 A. So the error obtained for the theoretical volume is typical for LDA methods within the DFT. These parameters were used during the structural factor's calculations. We have found that the bulk modulus is equal to about 12.49 Pa^{-1} which is in good agreement with experimental data $(12.89\ \mathrm{Pa})^{-1}$.[18]

A general view of the BABOH BS calculated within the method described above is presented in Fig. 2. One can see that the band dispersion $E(\mathbf{k})$ is rather flat and band level crossing is very low. Moreover, the observed **k** dispersion is similar both for the valence band states (see v.b.1 and v.b.2) as well as for the unoccupied conduction band states (c.b.1, c.b.2, c.b.3, c.b.4). Another important factor is an indirect type of the band energy gap E_g (the top of the VB is situated at the *R* BZ point and the bottom of the conduction band at the Γ BZ point). This is in accordance with the experimental measurements of the band energy type presented in Ref. 18, where steplike phonon repetitions were observed (which indicates an indirect absorption edge). Very close to the first maximum (about 0.1 eV below it), there is a second local valence BS maximum (near the *X* point of the BZ) and the bottom of the valence band (at the Γ point) corresponding to the local minimum of the valence band top. The calculated E_g is equal to about 5.22 eV and is only a little less from the experimentally measured 5.26 eV for the $\mathbf{E}\|\mathbf{b}$ light polarization. It is crucial that for $\mathbf{E}\|\mathbf{c}$ light polarization, the experimentally measured E_g is equal to about 5.67 eV.

In Table I our measured refractive indices of BaBOH are presented and a comparison with the BBO single crystals is done. One can see that birefringence (the difference between two principal refractive indices) is higher for BaBOH compared to BBO (0.17 and 0.12, respectively). This is an additional confirmation of the higher anisotropy of BaBOH compared to the BBO that are the more well-known highly anisotropic borates today.

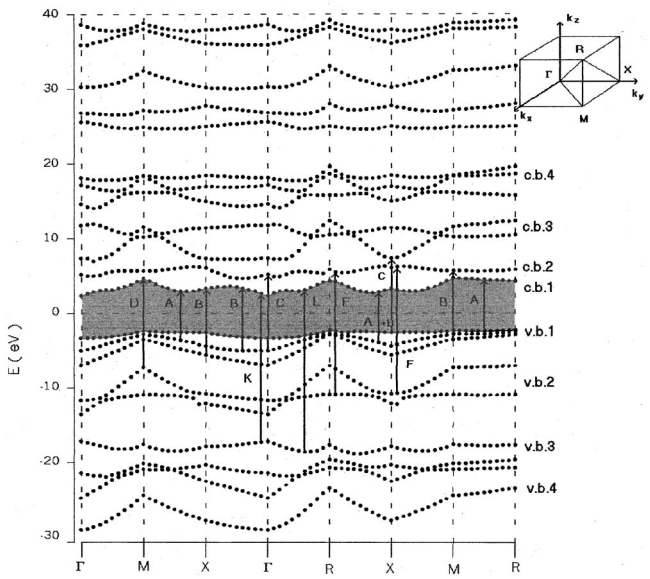

FIG. 2. Main symmetry points in the first BZ of BABOH single crystals and band structure calculated within the BHS model.

We carried out simulations of the imaginary part of dielectric susceptibility $\varepsilon_2(E)$ for the two light polarizations ($\mathbf{E}\|\mathbf{c}$ and $\mathbf{E}\|\mathbf{b}$) and compared the performed calculations with those obtained experimentally from the ellipsometric measurements. The corresponding results are presented in Fig. 3. From Fig. 3 one can clearly see that values of the $\varepsilon_2{}^{(b)}(E)$ are substantially higher than $\varepsilon_2{}^{(c)}(E)$ (here **b** and **c** correspond to the polarization of light along **b** and **c** crystallographic directions, respectively). Our calculations have shown that the main contribution to $\varepsilon_2{}^{(b)}(E)$ is in the M-Γ-X direction of the BZ. For $\varepsilon_2{}^{(c)}(E)$ the more prominent contribution seems to be in the *RM* direction. Γ*R* and *RX* BZ directions give contributions to both polarizations simultaneously. Our calculations have shown that the M-F-X BZ direction gives the number of optical interband transitions contributing to $\varepsilon_2(E)$ at least 40% higher than the *RM*. This one reflects the different number of interband transitions due to the different number of basic plane wave functions contributing to interband transitions in the **c** and **b** crystallographic directions. As a consequence we have the anisotropy in the values of $\varepsilon_2{}^{(b)}(E)$ and $\varepsilon_2{}^{(c)}(E)$.

For convenience, in the major interband transitions are indicated in Fig. 3. One can see that the major anisotropy is originated due to the *B* transitions (spectral range 6.2–7.4 eV). The *B* maxima are formed both due to the inter band transitions in the Γ-X-R BZ direction as well in the *MR* BZ direction (compare Figs. 2 and 3). The maxima **A** demonstrate similar behaviors for two polarizations and are slightly spectrally shifted. Depending on the relative contribution of the particular structural borate fragments to the BZ directions we have revealed that coordination's disturbance of oxygens

TABLE I. Principal refractive indices for the BaBOH and BBO single crystals.

Crystal	n_o	n_e	n_z	n_y
BaBOH			1.47($\lambda = 0.633$ nm)	1.62($\lambda = 0.633$ nm)
BaBOH			1.52($\lambda = 0.337$ nm)	1.69($\lambda = 0.337$ nm)
BBO (Ref. 19)	1.68($\lambda = 0.633$ nm)	1.55($\lambda = 0.633$ nm)		
BBO (Ref. 19)	1.71($\lambda = 0.337$ nm)	1.58($\lambda = 0.337$ nm)		

within the borate rings is not so crucial for the splitting of the BS levels for the BaBOH crystals as in the case of the BBO and LBO.[8,9] This is in agreement with the BZ splitting of the v.b.1 in the M-X-Γ-R and X-M BZ directions.

The main origin of the observed $\varepsilon_2(E)$ anisotropy is caused by different values of the projection of the bonding $2p_{x,y}$B-$2p_{x,y}$O states (forming prevailingly v.b.1 and v.b.2) on particular directions of the BZ due to the specific crystallochemistry of BaBOH (Fig. 1). The second group of levels (indicated by **D**, **E**, and **F**) are originated from the $5p$ Ba atoms (the lower part of v.b.2 and v.b.3), that analogously to the case of other borates[3,8,9] may be considered as corelike states that do not substantially disturb the crystalline anisotropy. As a consequence, we observe only changes of the values of $\varepsilon_2(E)$ maxima without a spectral shift for the mentioned spectral region.

One can also see that spectral positions of the energetically higher $\varepsilon_2(E)$ maxima show substantially better spectral coincidence between experiment and theory. The good similarity of the calculated and measured $\varepsilon_2(E)$ spectra may be seen in the adopted theoretical model.

For evaluations of the origin of the particular bands we have used the band-projection procedure from the plane wave basis set to the localized orbitals described in Ref. 14. In Fig. 4, the pseudocharge density distributions for different crystalline sequences are shown. One can see substantial anisotropy of the charge density distribution for the crystalline $\langle 110 \rangle$ cut [Fig. 4(a)] and $\langle 011 \rangle$ cut [Fig. 4(b)]. For convenience the cuts are done at the $c/2$ and $a/2$ planes and even without a charge density gradient calculation one can see a large charge density anisotropy.

V. DISCUSSION

Comparing the calculated band energy structure of BaBOH with the BS of other borates one can see substantial differences in the band's dispersion behavior compared to other borates.[8,3,9] The BaBOH crystals have larger BS dispersion, particularly for the Γ-R-X directions of the BZ. The performed calculations show that the latter is caused by substantial admixture of the covalence bonding-antibonding $2p$O-$2p$B chemical orbitals originating from the borate structural fragments giving different contributions in different BZ directions.

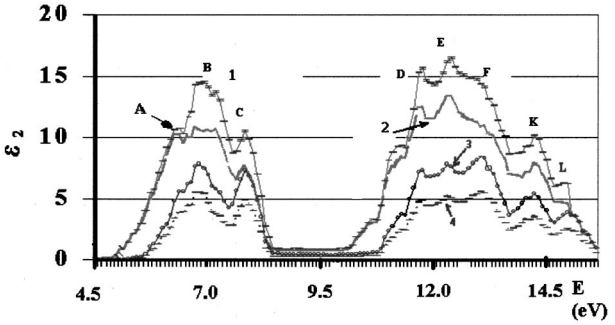

FIG. 3. Spectral dependencies of the imaginary part of dielectric susceptibility $\varepsilon_2(E)$. $\varepsilon_2{}^{(b)}$: (1) experimental; (2) theoretically calculated; $\varepsilon_2{}^{(c)}$: (3) experimental; (4) theoretically calculated.

Comparing with other borate crystals[8,3,9] it is also necessary to note that the general similarities between them are the relatively flat features of the valence band dispersion hence the total number of bands in the case of BaBOH is less because we have only two molecules per unit. In addition, the values of E_g are close (within 6.8–5.2 eV). This is a consequence of the common origin of all the band gaps in the borates (caused by $2p$O-$2p$B bonding-antibonding splitting). The relatively high **k** dispersion of the BABOH compared to other borates for the deeper corelike states originating from the $2s$O and 5 s,p Ba states is also interesting.

The appearance of the anisotropy is enhanced additionally by weak $2p_y$O-$2p_y$O antibonding bonds (similar to week van der Waals bonds) originating from oxygens belonging to the neighboring layers (see Fig. 1). The strong charge density anisotropy reflects an influence of the ions from up to the fourth coordination sphere on the intralayered barium-borate ionic-covalent bond components, contrary to the BBO where such anisotropy is caused prevailingly by different oxygen coordination within the covalent borate ring.

The space electron charge density gradient shows a huge level of anisotropy. For example, for the intramolecular band for the $\langle 110 \rangle$ BZ direction, this derivative is equal to 36 $[e/(\Omega\,\mathrm{A})]$ and for the direction $\langle 101 \rangle$ it is equal to 280 $e/(\Omega\,\mathrm{A})$. For comparison, the best known anisotropic crystals InBr have corresponding parameters equal to 45 and 217 $e/(\Omega\,\mathrm{A})$, respectively.[20] This fact indicates that in order to find new highly anisotropic borates it is necessary to modify the packing of the particular borate complexes in such a way as to achieve a large degree of anisotropy in orbital distributions. Only manipulation by oxygen within the borate rings or due to interlayer van der Waals forces is not sufficient enough for substantial enhancement of anisotropy. To obtain a space separation of particular borate planes it is necessary to have additional molecular groups favoring a separation of the mentioned borates. BaBOH plays such a role in OH groups, however, one can expect that materials engineering will search for other complexes useful for the achievement of the desired effects.

VI. CONCLUSIONS

Using self-consistent nonlocal norm-conserving pseudopotential calculations we have found a correlation between

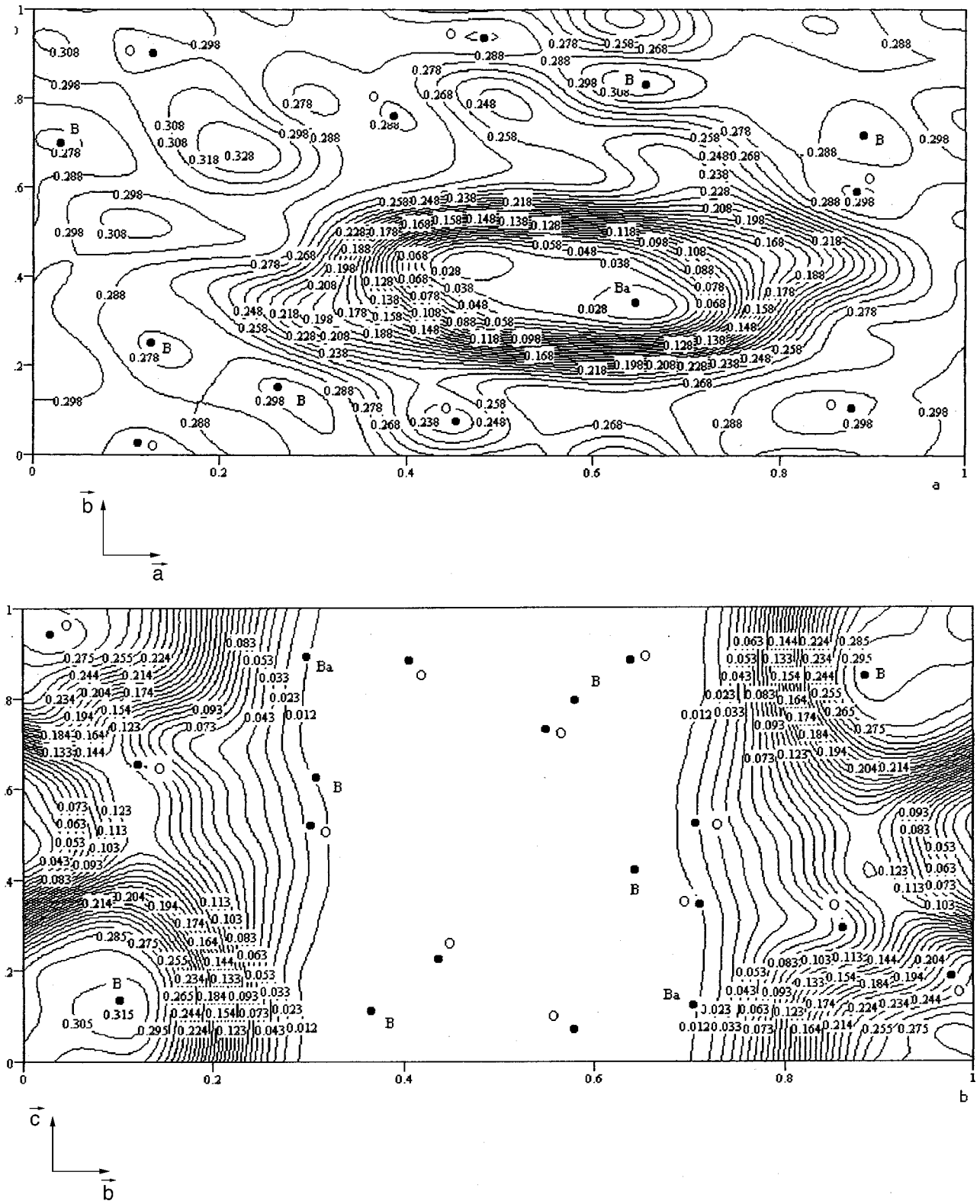

FIG. 4. Charge-density distribution in the BaBOH (a) on the ⟨110⟩ at $\mathbf{c}=0.5$; (b) on the ⟨011⟩ at $\mathbf{a}=0.5$. The contour lines are from 0.02 to 0.25 by 0.005 all in units/(a.u.)$^{-3}$.

the giant anisotropy of charge density, optical spectra, and corresponding chemical bonds.

Comparing the calculated BS of BaBOH with those of other borates, one can see substantial changes in the band's dispersion behavior. The BaBOH crystals have larger BS dispersion, particularly for the Γ-R-X directions of the BZ. The performed calculations show that this is caused by a substantial admixture of the covalence bonding-antibonding

$2p$O-$2p$B chemical orbitals originating from the structural clusters possessing different planes of borate rings in the BaBOH. As a consequence, the values of $\varepsilon_2{}^{(b)}(E)$ are substantially higher than the values of $\varepsilon_2{}^{(c)}(E)$.

Comparing with other borate crystals[8,3,9] it is necessary to note that the general similarities in them are the relatively flat features of the valence bands and close values of the energy gaps. Our calculations have shown that main contribution to $\varepsilon_2{}^{(b)}(E)$ is in the M-Γ-X direction of the BZ. For $\varepsilon_2{}^{(c)}(E)$ the more prominent contribution seems to be in the RM direction. The ΓR and RX BZ directions give contributions to both $\varepsilon_2(E)$ polarizations. Our calculations have shown that the M-F-X BZ direction gives a number of optical interband transitions that is at least 40% higher than for the RM ones. In the optical spectra, major anisotropy is caused by the interband optical transitions within spectral range 6.2–7.4 eV because the corresponding maxima are formed both due to the transitions in the Γ-X-R BZ direction as well as in the MR BZ direction. Other spectral maxima demonstrate similar features for two light polarizations and are only spectrally shifted.

We have evaluated that different local positions of oxygens within the borate rings is not so crucial for the splitting of the band levels (origin of the observed anisotropy) for the BaBOH as in the case of the BBO. The higher energy maxima (within the 10.5–15 eV) are originated from the $5p$ Ba states are similar to other borates[8,9,3] and may be considered as corelike states that do not disturb the crystalline anisotropy. A good similarity of the calculated and measured $\varepsilon_2(E)$ spectra may show in the adopted theoretical model.

[1] L. K. Cheng, W. Bosenberg, and C. L. and Tang, J. Cryst. Growth **89**, 553 (1988).

[2] C. T. Chen, Y. Wu, A. Jiang, B. Wu, G. You, R. Li, and S. Lin, J. Opt. Soc. Am. B **6**, 616 (1989); C. T. Chen, B. C. Wu, and A. D. Jiang, Sci. Sin., Ser. B (Engl. Ed.) **28**, 234 (1985).

[3] I. V. Kityk and A. Mefleh, Physica B **262**, 172 (1999); I. V. Kityk, P. Smok, J. Berdowski, T. Łukasiewicz, and A. Majchrowski, Phys. Lett. A **280**, 70 (2001).

[4] Y. Mori, I. Kuroda, T. Sasaki, and S. Nakai, Jpn. J. Appl. Phys. **34**, L296 (1995).

[5] G. Zhang, Y. Wu, P. Fu, G. Wang, H. Liu, G. Fan, and C. Chen, J. Phys. Chem. Solids **63**, 145 (2002).

[6] G. Aka, A. Kahn-Haradi, D. Vivien, J.-M. Benitez, F. Salin, and J. Godard, Eur. J. Solid State Inorg. Chem. **33**, 727 (1996); I. N. Ogorodnikiov, V. A. Pustovarov, A. V. Kruzhalov, L. I. Isaenko, M. Kirm, and G. Zimmerer, Phys. Solid State **42**, 1846 (2000).

[7] P. Becker, Adv. Mater. **10**, 979 (1998).

[8] R. H. French, J. W. Ling, F. S. Ohuchi, and C. T. Chen, Phys. Rev. B **44**, 8496 (1991).

[9] Y.-N. Xu, W. Y. Ching, and R. H. French, Phys. Rev. B **48**, 17 695 (1993).

[10] D. Yu. Pushcharowsky, S. Merlino, O. Ferro, S. A. Vinogradova, and O. V. Dimitrova, J. Alloys Compd. **306**, 163 (2000).

[11] M. A. Simonov, O. G. Karpov, G. K. Shvirkst, and G. K. Gode, Sov. Phys. Crystallogr. **34**, 1292 (1989).

[12] G. B. Bachelet, D. R. Hamann, and M. Schluter, Phys. Rev. B **26**, 4199 (1982).

[13] G. Wusger, *Structural Data* (German Structural Society, Berlin 1999), Vol. 24, p. 124.

[14] I. V. Kityk, B. V. Andriewskii, and J. Kasperczyk, Phys. Lett. A **216**, 161 (1996).

[15] J. B. Perdew and A. Zunger, Phys. Rev. B **23**, 5048 (1981).

[16] D. M. Ceperley and B. J. Adler, Phys. Rev. Lett. **45**, 161 (1980).

[17] D. J. Chadi and M. L. Cohen, Phys. Rev. B **8**, 5747 (1973).

[18] S. G. Simonenko and I. Q. Sergeev, Cryst. Phys. 6, 156 (1998).

[19] J. T. Lin, Proc. Soc. Photo-Opt. Instrum. Eng. 162 (1988).

[20] M. Kolinko and O. Bowhiry, Bull Lviv Univ. Ser. Phys. **33**, 21 (2000).